Article

Over-Expression of Larch *DAL1* Accelerates Life-Cycle Progression in *Arabidopsis*

Zha-Long Ye, Qiao-Lu Zang, Dong-Xia Cheng, Xiang-Yi Li, Li-Wang Qi and Wan-Feng Li *

State Key Laboratory of Tree Genetics and Breeding, Key Laboratory of Tree Breeding and Cultivation, National Forestry and Grassland Administration, Research Institute of Forestry, Chinese Academy of Forestry, Beijing 100091, China; kemiye@caf.ac.cn (Z.-L.Y.); zangql@sxau.edu.cn (Q.-L.Z.); cdx@caf.ac.cn (D.-X.C.); lixiangyi@caf.ac.cn (X.-Y.L.); lwqi@caf.ac.cn (L.-W.Q.)

* Correspondence: liwf@caf.ac.cn; Tel.: +86-10-62889628; Fax: +86-10-62872015

Abstract: Homologs of *Larix kaempferi DEFICIENS-AGAMOUS-LIKE 1* (*LaDAL1*) promote flowering in *Arabidopsis*. However, their functional role in the whole life-cycle is limited. Here, we analyzed the phenotypes and transcriptomes of *Arabidopsis* plants over-expressing *LaDAL1*. With respect to the defined life-cycle stage of *Arabidopsis* based on the meristem state, the results showed that *LaDAL1* promoted seed germination, bolting, flower initiation, and global proliferative arrest, indicating that *LaDAL1* accelerates the meristem reactivation, the transitions of vegetative meristem to inflorescence and flower meristem, and meristem arrest. As a marker gene of meristem, *TERMINAL FLOWER 1* was down-regulated after *LaDAL1* over-expression. These results reveal that *LaDAL1* accelerates the life-cycle progression in *Arabidopsis* by promoting the transition of meristem fate, providing more and novel functional information about the conifer age-related gene *DAL1*.

Keywords: *AGL6*; gymnosperm; life-cycle; lifetime; MADS-box; reproductive development

1. Introduction

In the life cycle of plants, seedlings start vegetative growth after seed germination. As time goes on, they enter the reproductive phase and can flower and produce seeds. The life cycle recurs in the next generation (Figure 1). In *Larix kaempferi* (Japanese larch), ~10 years are needed for one life cycle, and ~20 years in *Picea abies*. The timing of life-cycle events is important for forestry, because it determines the efficiency of breeding and seed production. So, studying the mechanisms underlying life-cycle progression is of great relevance and economic value.

Comparative transcriptomic analysis has been performed in *L. kaempferi*, *Pinus tabuliformis* Carri. and *Pinus koraiensis* Sieb. & Zucc. to reveal the molecular basis of the conifer reproductive phase change [1–3]. Differentially expressed genes have been identified, and a regulatory network model has been proposed for *L. kaempferi* based on these genes [3]. Among them, *L. kaempferi DEFICIENS-AGAMOUS-LIKE 1* (*LaDAL1*, also named *LaAGL2-1*, GenBank accession number: MN790744), a MADS-box transcription factor and a homolog of *Arabidopsis thaliana* (L.) Heynh. *AGL6*, is controlled by age [3,4], because its transcript level is low before 5 years and then maintained at a high level after 5 years of age. This age-dependent pattern is conserved in *P. abies* [5], *P. koraiensis* [2] and *P. tabuliformis* [1], indicating that at ~5 years, some conserved and unknown life-cycle events occur in these trees [3]. Furthermore, over-expression of *P. abies* (L.) H.Karst. *DAL1* (*PaDAL1*) [5], *Cryptomeria japonica* (Thunb. ex L.f.) D.Don *CjMADS14* (a homolog of *DAL1*) [6], and *P. tabuliformis DAL1* (*PtDAL1*) [1] in *A. thaliana* results in early flowering. These data indicate that *LaDAL1* and its homologs may be regulators of life-cycle progression, but whether they can regulate other life-cycle events in addition to flowering is still unknown.
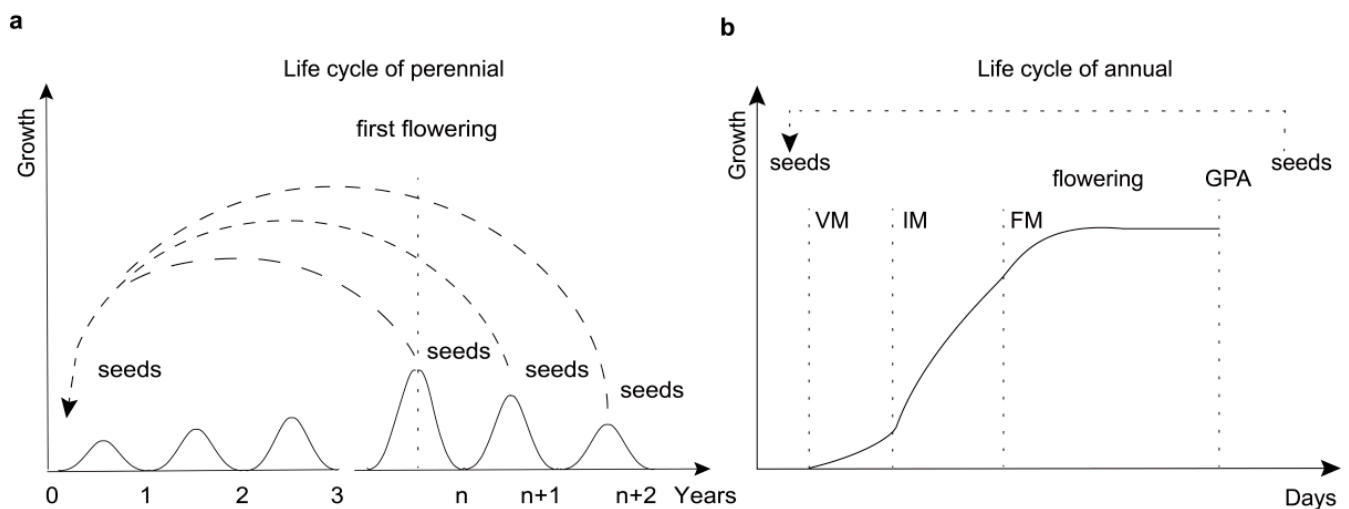
Figure 1. The life-cycle progression model in perennials and annuals. (**a**) The life-cycle progression in perennials such as *Larix kampferi*. (**b**) The life-cycle progression in annuals such as *Arabidopsis thaliana*. VM, vegetative meristem; IM, inflorescence meristem; FM, flower meristem; GPA, global proliferative arrest. Vertical dotted lines indicate times of meristem formation and activtiy.

Compared with perennial plants (Figure 1a), the life cycle revolves faster in *A. thaliana* and life-cycle events are easily recorded with meristem fate transition (Figure 1b). Specifically, rosette leaves develop in a specific order with the activity of vegetative meristem. When rosette leaves reach a certain number, the vegetative meristem transforms into inflorescence meristem, and a stem-like structure named the inflorescence axis is produced. This process is often called bolting. After bolting, cell division in shoot apical meristem (SAM) in the inflorescence axis keeps going and results in the inflorescence axis growing upward [7–10]. Axillary meristem exists at the axil of the cauline leaf, and its activity leads to the growth of lateral branches. In the growth process of the inflorescence axis and lateral branches, inflorescence meristem develops into flower meristem, and flower meristem subsequently develops into flowers. After the formation of a specific number of siliques, cell division in the SAM is arrested, and flower meristem is not produced and finally turns into silique [11]. This phenomenon is defined as global proliferative arrest (GPA) [12–15]. The whole plant senesces and dries up, silique dehiscence occurs, and seeds fall. At this point, one life cycle is over, and the next one recurs in offspring with seed germination (Figure 1b).

The timing of *A. thaliana* life-cycle events such as bolting and flowering has been widely studied and controlled genetically [16]. For this reason, *A. thaliana* is often used to determine the functions of genes from woody perennial plants [1,17]. Here, we overexpressed *LaDAL1* in *A. thaliana* and provided morphological and genetic evidence that *LaDAL1* accelerates life-cycle progression by promoting the transition of meristem fate.

2. Materials and Methods

2.1. Plant Materials and Growth Conditions

The seeds of *A. thaliana* ecotype Columbia (Col-0) saved in our laboratory were disinfected in 0.9% NaClO solution and then inoculated onto 1/2 Murashige and Skoog medium. After being kept at 4 °C for 3 days, seeds were grown under a 16 h photoperiod at 22 °C with 40% relative humidity. When the seedlings had 2–3 true leaves, some were sown in 1:1 mixed roseate and nutrient soil and some were sampled for genomic DNA and total RNA extraction. All of the samples were immediately frozen in liquid nitrogen and then stored at −80 °C.

2.2. Plasmid Construction and Genetic Transformation

LaDAL1 was cloned in our previous work [4]. In this study, its full-length coding sequence was cloned into the binary vector pCAMBIA1305.1, resulting in the *CaMV35S::LaDAL1* vector, and then this vector was transformed into *A. thaliana* ecotype Col-0 with the floral dip method mediated by the *Agrobacterium tumefaciens* strain GV3101. T1 transformants were selected on kanamycin (50 mg/L, Sigma, Saint Louis, MO, USA) Luria-Bertani culture plates. T2 transgenic plants before bolting were sampled for RNA-seq. Homozygous T3 transgenic plants were analyzed by polymerase chain reaction (PCR) and quantitative reverse transcription PCR (qRT-PCR) and then used for phenotypic observation.

2.3. The Extraction of Nucleic Acid, PCR, and qRT-PCR

Genomic DNA was extracted from *A. thaliana* using the Plant Genomic DNA Kit (TIANGEN, Beijing, China). The transgenic T3 seedlings were analyzed by PCR with the specific primers 5′-ATGGGGCGGGGGCGAGTCCAGC-3′ and 5′-AATCCACCAGCCTTGCATGTAT TGG-3′. The transgenic T3 seedlings were also analyzed by qRT-PCR. Total RNA was extracted using the EasyPure RNA Kit (TransGen Biotech, Beijing, China) according to the manufacturer's instructions. A 2.5 µg aliquot of total RNA was reverse-transcribed into cDNA with the TransScript II One-step gDNA Removal and cDNA Synthesis SuperMix Kit (TransGen Biotech, Beijing, China), and subsequently diluted for gene expression analysis. qRT-PCR analysis was performed on a Bio-Rad CFX96 PCR system, using a TB Green$^{®}$ Premix Ex Taq™ (Tli RNase H Plus) (Takara, Shiga, Japan). Each reaction was carried out on 2 µL of diluted cDNA sample, in a total reaction system of 25 µL. The following program was used: 30 s 95 °C, 40 cycles (5 s 95 °C, 30 s 60 °C). The specific primers 5′-AACGCAGGTGATGCTAGACC-3′ and 5′-CCAAGGCCCGTTAGTACCAG-3′ were used for *LaDAL1*. *AtUBQ1* (AT3G52590) was used as an internal control [18] with the specific primers 5′-GCCAAGATCCAAGACAAAGAAG-3′ and 5′-CTGATTGTACTTACGAGCAAG C-3′. The relative gene expression levels were calculated from $2^{-\Delta\Delta Ct}$ values. qRT-PCR was performed with three biological replicates, and data are shown as the mean $\pm$ SD.

2.4. Phenotypic Observation and Statistical Analysis

Several phenotypic indexes were measured in wild-type and transgenic *A. thaliana* plants, including the germination rate, the bolting time, first flowering time, the time of formation of the last flower in the principal inflorescence axis, the number of siliques, the number of rosette leaves and branches, and the length of the inflorescence axis. Thirty seeds were used in each line for the germination rate analysis. At least 15 independent individuals in each line were used, and a repeat experiment was conducted. GraphPad Prism 9 and the R packages ggplot2, ggsignif, ggpubr, and RColorBrewer were used for the statistical analysis and graphics. The significance of differences between *LaDAL1* transgenic lines and wild-type *A. thaliana* were analyzed by Student's *t*-tests.

2.5. Transcriptome Analysis

cDNA library construction and RNA-seq were performed by Sangon Biotech (Shanghai, China) following standard protocols and sequenced on an Illumina HiSeq 2000 platform; 150-bp paired-end reads were generated. FastQC (http://www.bioinformatics.babraham. ac.uk/projects/fastqc, accessed on 16 March 2020) and Trimmomatic v.0.30 [19] were used for initial quality control, and the raw reads were filtered to remove reads consisting of adapters, reads containing runs of poly-Ns (unknown bases) and low-quality reads to give clean reads. At the same time, the Q20 and Q30 scores, the GC-contents, and the level of sequence duplication in the clean data were calculated for each sample. All clean reads were aligned to the reference genome of *A. thaliana* (*A. thaliana* TAIR 10 genome). Fragments Per Kilobase of transcript per Million mapped reads was calculated to evaluate the transcriptional levels of genes [20].

Differential expression analysis between wild-type and transformed *A. thaliana* was performed using DESeq2 v1.26 [21]. Genes with $|\log2\text{FoldChange}| \geq 1$ and *q* value < 0.05 [22]

were identified as differentially expressed genes (DEGs). The annotations of DEGs were obtained from TAIR (https://www.arabidopsis.org/, accessed on 16 March 2020). Heatmaps were used to show the change of expression levels using TBtools [23]. Log scales and row scales were used to display the change of pattern between groups.

3. Results and Discussion

3.1. Successful Transformation of LaDAL1 into A. thaliana

In total, 12 T1 transgenic *A. thaliana* lines were obtained, seven of which (D3, D4, D5, D7, D8, D9, and D10) were randomly selected for further experiments. To verify the insertion of *LaDAL1* in the *A. thaliana* genome, we purified genomic DNA and carried out PCR amplification. Genomic DNA from wild-type *A. thaliana* was also extracted and used as control. We detected *LaDAL1* in these seven transgenic lines and not in the wild-type (Figure 2a), indicating that *LaDAL1* was successfully integrated into the genome of *A. thaliana*.
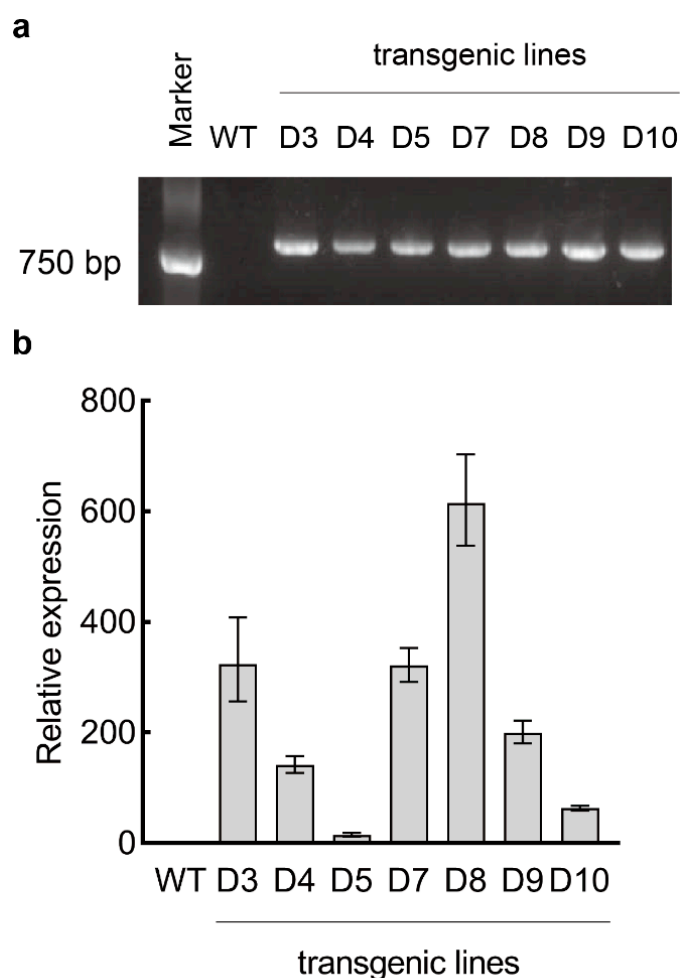

Figure 2. Verification of transgenic *Arabidopsis thaliana*. (**a**) PCR amplification of *LaDAL1* from wild-type (WT) and transgenic genomic DNA. (**b**) Relative expression levels of *LaDAL1* measured by qRT-PCR with *AtUBQ1* as the internal control.

To detect the expression of *LaDAL1*, total RNA was extracted and qRT-PCR was carried out. We detected transcripts of *LaDAL1* in these seven transgenic lines and not in the wild-type *A. thaliana* (Figure 2b). Based on these results, these seven lines were used for morphological observation and phenotypic analysis.

3.2. LaDAL1 Over-Expression Accelerates the Reactivation of Meristem

LaDAL1 over-expression increased the germination rate of *A. thaliana* seeds (Figure 3), because on the fourth day after 4 °C treatment, 83.8% of transgenic seeds germinated, while only 46.7% of wild-type seeds germinated (Figure 3b), indicating that the meristem reactivation from dormancy is promoted by *LaDAL1* over-expression.
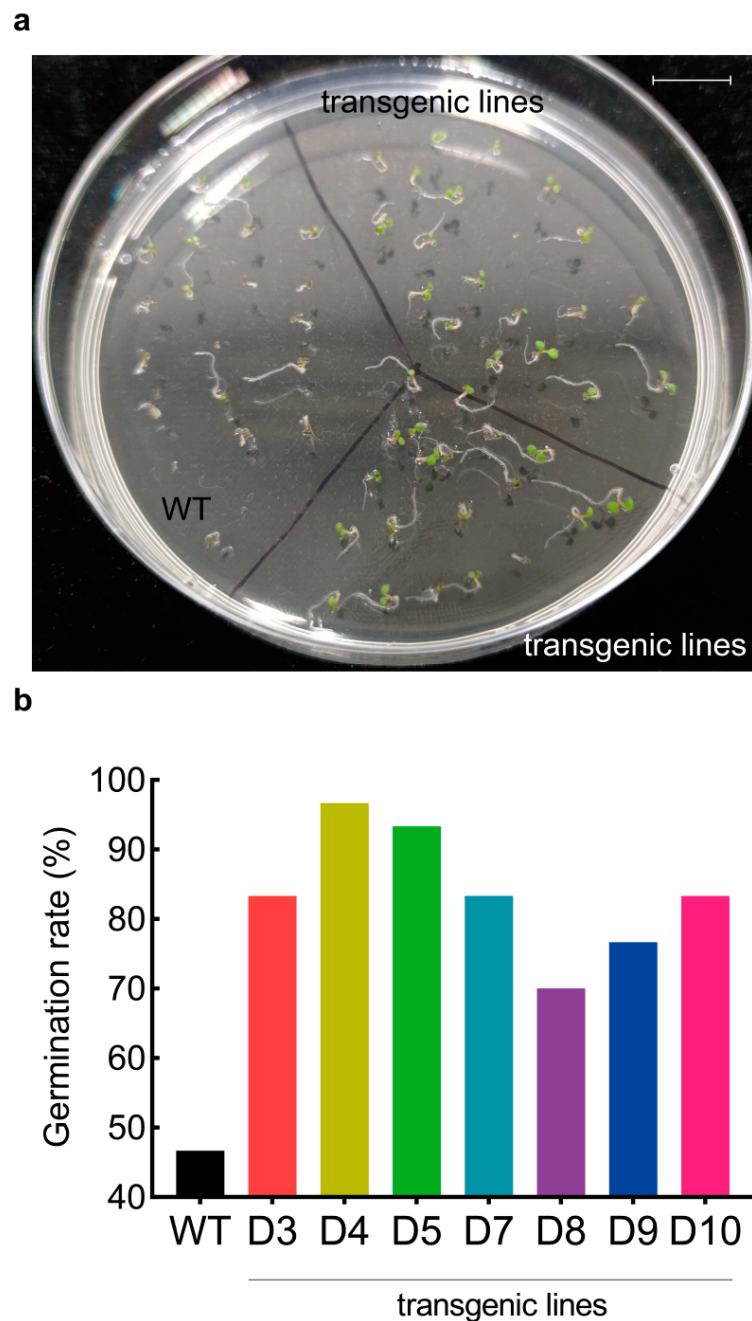
a

b

Figure 3. Germination rate of wild-type and *LaDAL1* over-expressing *Arabidopsis thaliana*. (**a**) Images of wild-type and transgenic plants. Bar 1 cm. (**b**) Germination rate of wild-type and transgenic plants on the fourth day after 4 °C treatment. Thirty seeds were used in each line. When two cotyledons were visible, germination was counted.

3.3. LaDAL1 Over-Expression Accelerates the Transition of Meristem Fate

After measuring the bolting time and the number of rosette leaves in both transgenic and wild-type *A. thaliana*, we found that bolting was promoted by over-expression of

LaDAL1 (Figure 4a), because the bolting time of transgenic *A. thaliana* was reduced. For the wild-type, ~17.0 days were needed to bolt, while for transgenic *A. thaliana*, ~10.8 days were needed (Figure 4b). In addition, fewer rosette leaves were produced in transgenic *A. thaliana* (Figure 4c). In conclusion, transgenic *A. thaliana* had a shorter bolting time and fewer rosette leaves than the wild-type, indicating that the transition from vegetative meristem into inflorescence meristem is promoted by *LaDAL1* over-expression.
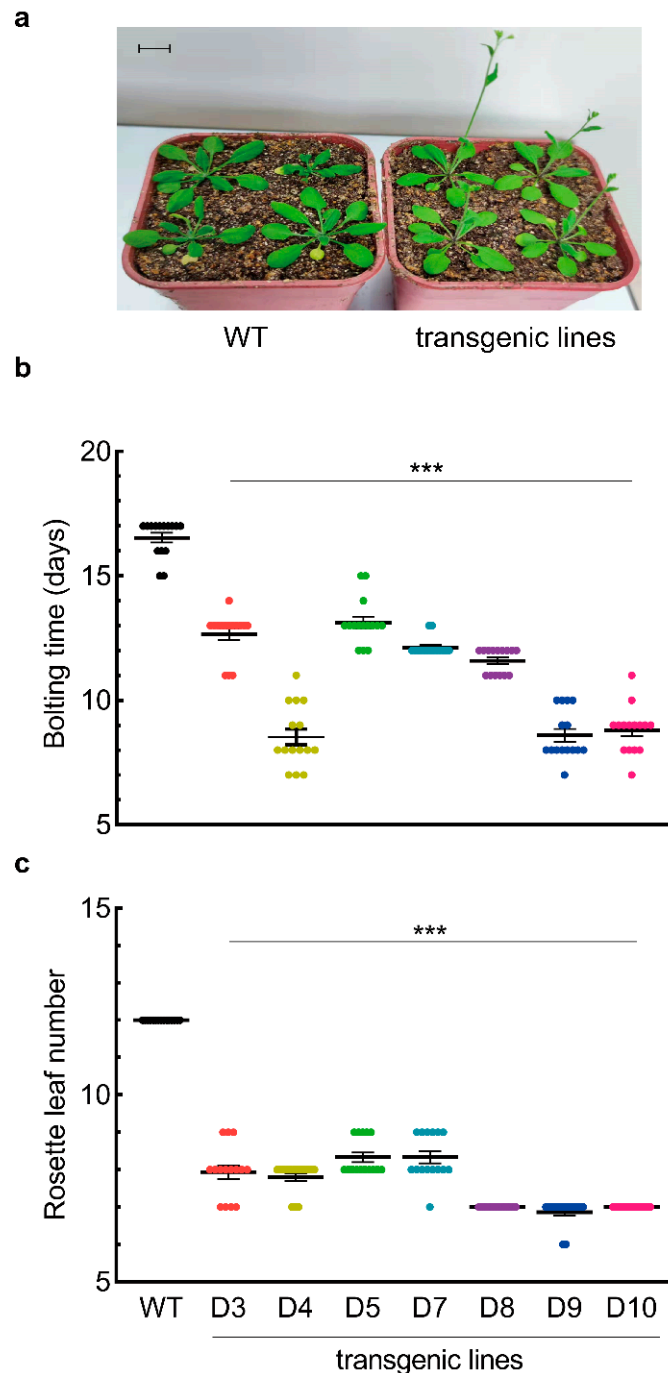

Figure 4. Bolting time and number of rosette leaves of wild-type and *LaDAL1* over-expressing *Arabidopsis thaliana*. (**a**) Images of wild-type and transgenic plants. Bar 1 cm. (**b**) Bolting time of wild-type and transgenic plants. (**c**) Rosette leaf number of wild-type and transgenic plants. Error bars, SE. When the length of the inflorescence axis was ~1 cm, bolting time and number of rosette leaves were counted. At least 15 independent individuals in each line were used. *** $p \leq 0.001$, Student's *t*-test.

To evaluate the initiation of flower meristem, we counted the time of first flower formation. It took the wild-type ~19 days to produce the first flower, while it took transgenic *A. thaliana* 14–17 days (Figure 5a,b), indicating that transgenic *A. thaliana* started flowering earlier than the wild-type, and *LaDAL1* over-expression results in the early initiation of flower meristem.
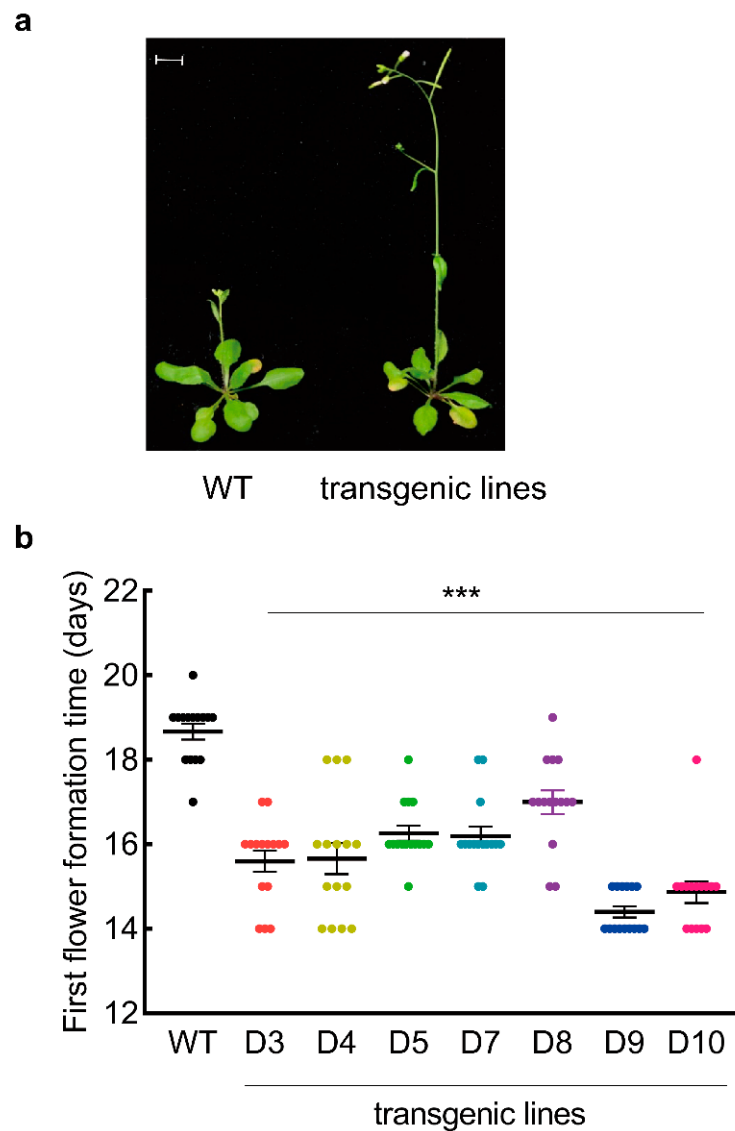
Figure 5. Flowering time of wild-type and *LaDAL1* over-expressing *Arabidopsis thaliana*. (**a**) Images of wild-type and transgenic plants. Bar 1 cm. (**b**) First flower formation time in wild-type and transgenic plants. At least 15 independent individuals in each line were used. Error bars, SE. *** $p \leq 0.001$, Student's *t*-test.

3.4. LaDAL1 Over-Expression Promotes GPA in A. thaliana

In the principal inflorescence axis, with the production of the last flower, SAM enters a state similar to dormancy, a spherical structure is formed in the apex of the inflorescence axis (Figure 6a), and inflorescence stays indeterminate [11]. Notably, indeterminate inflorescence can be changed into determinate inflorescence when a terminal flower is produced. For example, this occurs after the loss-of-function of *TFL1* or over-expression of *PaDAL1* and *PtDAL1* in *A. thaliana* [1,5,24]. However, a terminal flower was not observed in the seven *A. thaliana* lines over-expressing *LaDAL1* in our experiments.
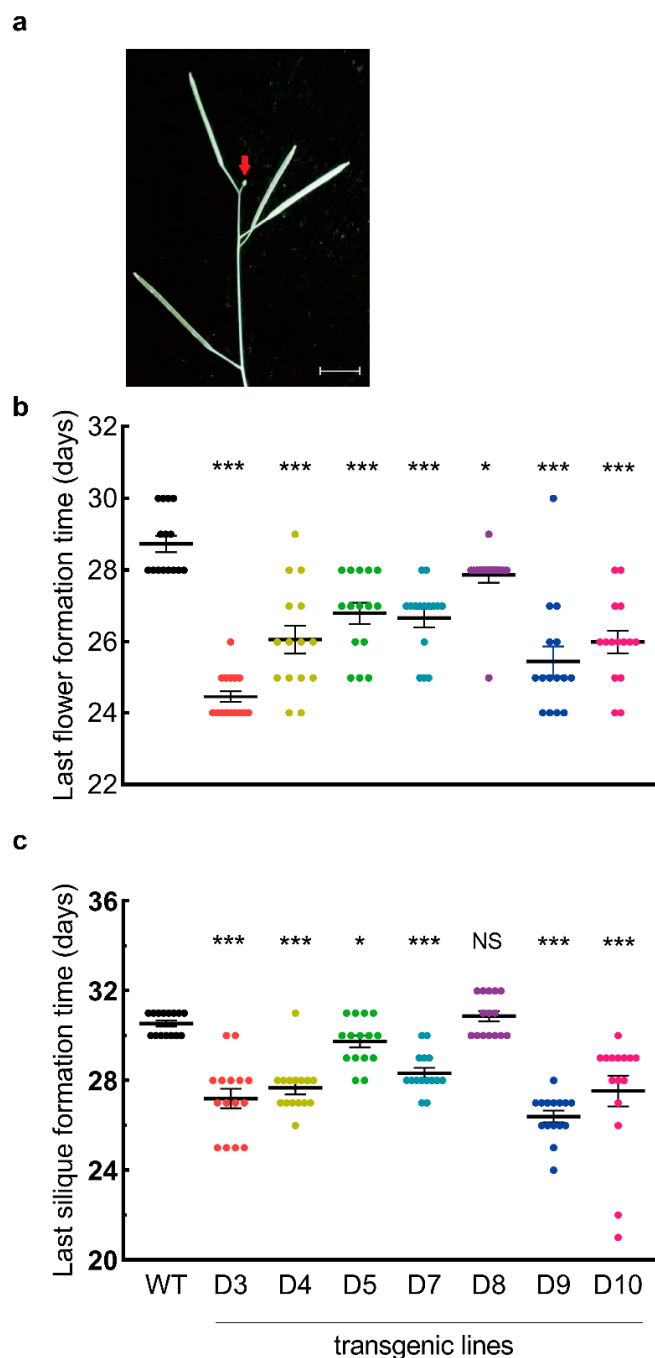
Figure 6. Formation of the last flower in the principal inflorescence axis and the last silique in wild-type and *LaDAL1* over-expressing *Arabidopsis thaliana*. (**a**) Image of the spherical structure (red arrow) formed at the apex of the principal inflorescence axis. Bar 5 mm. (**b**) Last flower formation time in the principal inflorescence axis in wild-type and transgenic plants. (**c**) Last silique formation time in wild-type and transgenic plants. At least 15 independent individuals in each line were used. Error bars, SE. *** $p \leq 0.001$, * $p \leq 0.05$, NS $p > 0.05$, Student's *t*-test.

In addition, we recorded the time of formation of the last flower in the principal inflorescence axis and found that it occurred earlier in transgenic *A. thaliana*. In the wild-type, ~29 days were needed, while for transgenic *A. thaliana*, ~26 days were needed (Figure 6b), indicating that *LaDAL1* over-expression promotes the formation of the last flower in the principal inflorescence axis and the entry of the SAM into arrest.

When the number of siliques stops increasing, GPA occurs in *A. thaliana* [14,25]. To assess the influence of *LaDAL1* over-expression on GPA, we counted the number of siliques every day until it did not increase. We found that it stopped increasing at ~31 days in the wild-type and at ~28 days in transgenic *A. thaliana* (Figure 6c), indicating that *LaDAL1* over-expression promotes GPA in *A. thaliana*.

3.5. LaDAL1 Over-Expression Influences the Inflorescence Architecture and Fruit Yield of A. thaliana

The architecture of *A. thaliana* also results from the activity of SAM. We found that fewer branches were produced in transgenic *A. thaliana*. There were 1–2 branches in 90.4% transgenic seedlings and no branches were produced in D9 and D10 lines, while 53.3% of wild-type seedlings had 3 branches (Figure 7a). In addition, the length of the principal inflorescence axis was shorter in 95.2% of transgenic *A. thaliana* (Figure 7b). The shorter inflorescence axes with fewer branches also occurred in transgenic *A. thaliana* after over-expression of *PaDAL1* and *PtDAL1* [1,5]. These results indicated that the architecture of *A. thaliana* is altered by over-expression of *DAL1* homologs.
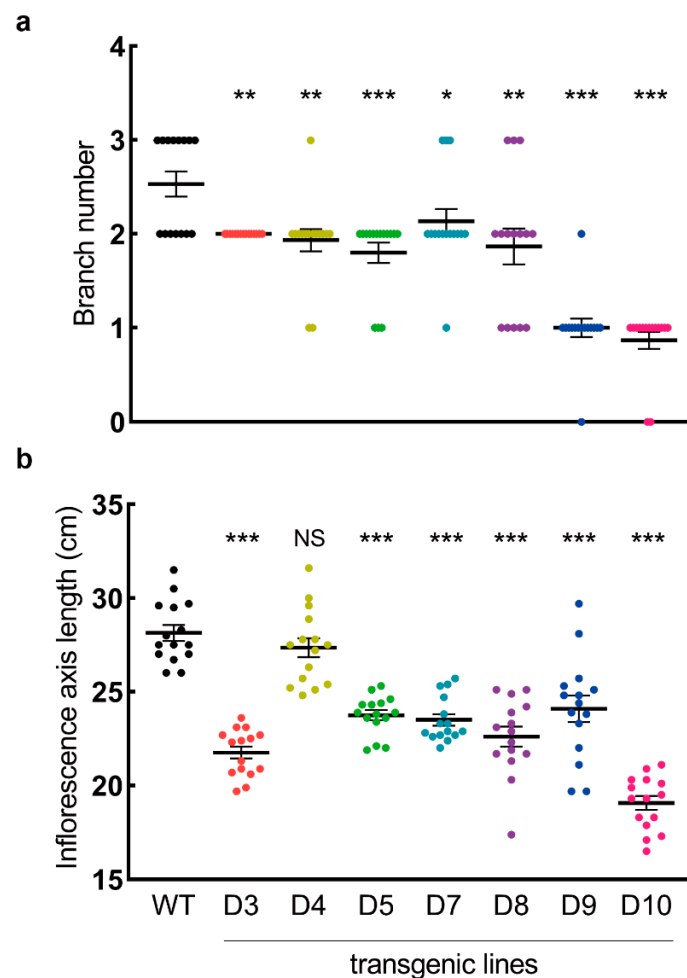

Figure 7. Number of branches and length of the inflorescence axis of wild-type and *LaDAL1* over-expressing *Arabidopsis thaliana*. (**a**) Branch number in wild-type and transgenic plants. (**b**) Inflorescence axis length in wild-type and transgenic plants. Error bars, SE. When the growth stopped, the number of branches and length of the inflorescence axis were counted. At least 15 independent individuals in each line were used. *** $p \leq 0.001$, ** $p \leq 0.01$, * $p \leq 0.05$, NS $p > 0.05$, Student's *t*-test.

Fruit yield is an important agronomic trait that is determined by many factors, such as the duration of inflorescence meristem activity, branch number, and fertility. To assess the global influence of *LaDAL1* over-expression on fruit production, we analyzed the total

number of siliques in *A. thaliana*. There were ~28 siliques in wild-type seedlings, while in transgenic seedlings the number was 8–42 (mean ± SD, 24.4 ± 6.5) (Figure 8), indicating that *LaDAL1* over-expression influences the production of siliques, and this influence is different in each transgenic *A. thaliana* line (the number of siliques in each line was different). As to the mechanism underlying this influence, we speculated that the duration of inflorescence meristem activity, branch number, and fertility are involved based on our findings and those of others [1,5]. Here, we did not check the fertility of transgenic *A. thaliana*, but a decrease in fertility resulting from heteromorphosis has been reported in *A. thaliana* after over-expression of *PaDAL1* and *PtDAL1* [1,5].
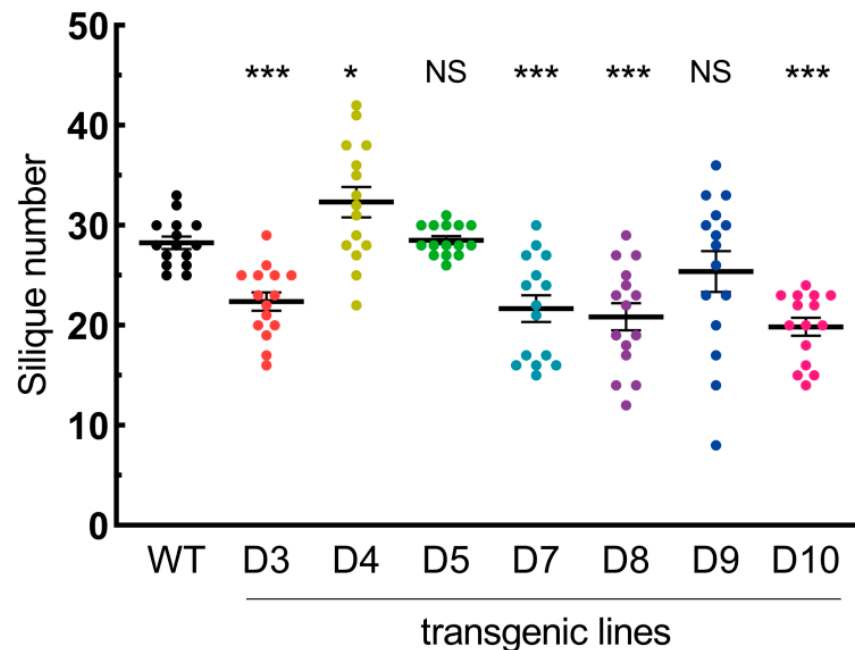

Figure 8. Silique number in wild-type and *LaDAL1* over-expressing *Arabidopsis thaliana*. At least 15 independent individuals in each line were used. Error bars, SE. *** $p \leq 0.001$, * $p \leq 0.05$, NS $p > 0.05$, Student's *t*-test.

3.6. LaDAL1 Over-Expression Changes the Expression of Genes Related to Aging

To understand how *LaDAL1* influences the life-cycle progression in *A. thaliana*, we analyzed the transcriptomic response to its over-expression. Comparative transcriptomic analysis was applied with four transgenic *A. thaliana* lines and wild-type seedlings. A total of 619 DEGs were identified, among which 398 were down-regulated by *LaDAL1* over-expression and 221 were up-regulated (Table S1). Based on the DEG annotation, we identified genes associated with life-cycle events. For example, *TEMINAL FLOWER 1* (*TFL1*), a key regulator of flowering time and the development of the inflorescence meristem [26,27], showed almost undetectable expression levels in transgenic *A. thaliana* and stronger expression in the wild-type (Figure 9); *AGAMOUS-like 24* [28], *AGAMOUS-like 42* [29], *MYB13* [30], and *ethylene response DNA-binding factor 3* [31], which regulate the floral process, were also down-regulated in transgenic *A. thaliana* (Figure 9); in addition, genes related to leaf senescence, such as *senescence-associated gene* [32,33], *dehydration-responsive element binding* and *EAR motif protein* [34], were up-regulated in transgenic *A. thaliana* (Figure 9). These data suggested that *LaDAL1* over-expression changes the transcriptome of *A. thaliana*, contributing to the acceleration of its life-cycle progression.
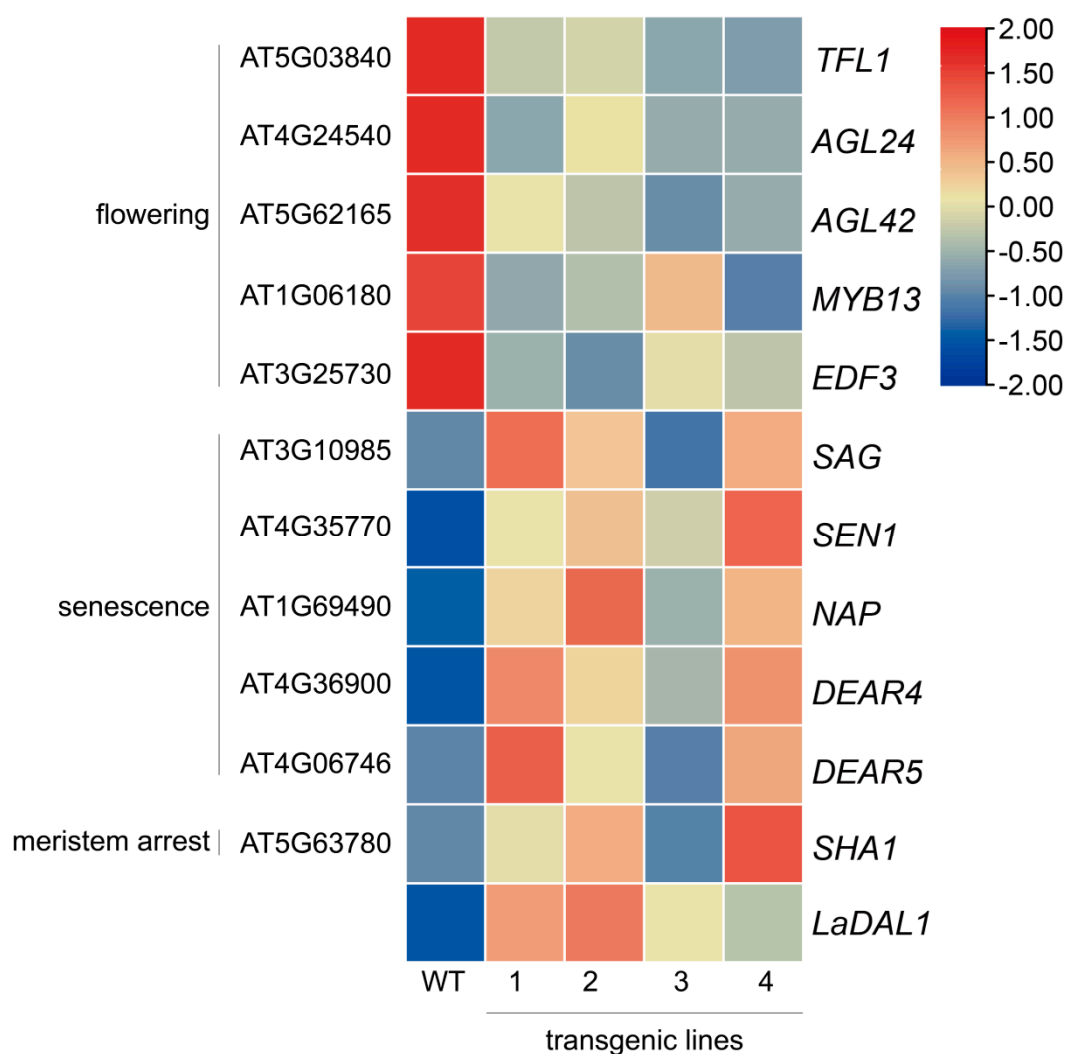
Figure 9. Heatmap showing the expression patterns of genes associated with *Arabidopsis thaliana* life-cycle events assayed by RNA-seq. The color scale (2 to −2) represents the values after being log-scaled and row-scaled with Fragments Per Kilobase of transcript per Million mapped reads.

3.7. LaDAL1 Over-Expression Accelerates Life-Cycle Progression in A. thaliana and Shortens Its Lifetime, Likely by Down-Regulating TFL1 Expression

In this work, we found that several life-cycle events in addition to flowering were promoted by *LaDAL1* over-expression. The early seed germination of transgenic *A. thaliana* showed that the reactivation of meristem from dormancy is promoted by *LaDAL1* over-expression. The decrease in bolting time and the number of rosette leaves showed that the transition of vegetative meristem to florescence meristem is promoted, and this has also been reported after over-expression of *PaDAL1* and *PtDAL1* [1,5]. We found early appearance of the first flower in *A. thaliana* over-expressing *LaDAL1*, indicating that the formation of flower meristem is also promoted. Notably, we found that the formation of the last flower in the principal inflorescence axis and GPA are also promoted by *LaDAL1* over-expression. In the annual plant *A. thaliana*, the occurrence of GPA means the end of its life. So, we conclude that *LaDAL1* over-expression accelerates the life-cycle progression in *A. thaliana* and shortens its lifetime. Altogether, our findings present more and novel functional information about conifer *DAL1*.

TFL1, a phosphatidyl ethanolamine-binding protein family gene, is a key regulator of flowering time and plant architecture. Its over-expression delays flowering, prolongs the length of the vegetative phase, and, in the *tfl1* mutant, there is an earlier flowering time, fewer rosette leaves and branches, and a shorter inflorescence axis with the formation of

a terminal flower [24]. These findings indicate that *TFL1* functions to maintain the fate of vegetative meristem and maintain the juvenility of the plant. In our study, *TFL1* was down-regulated after *LaDAL1* over-expression, and some phenotypes were similar to the *tfl1* mutant [27], indicating that down-regulation of *TFL1* by *LaDAL1* plays an important role in the transition of meristem fate and acceleration of *A. thaliana* life-cycle progression. However, whether *LaDAL1* regulates *TFL1* directly, and whether it also occurs in larch need further verification.

Modulation of life-cycle progression via changing *TFL1* expression with genetic transformation methods has been realized in some woody perennial plants [35]. In *Malus* [36–39], *Pyrus* [40,41], and *Populus* [42], the vegetative phase is markedly shortened and precocious flowering indeed occurs by down-regulating *TFL1* expression. Notably, *TFL1*-like genes from *P. abies* [43], *P. wilsonii* [44], and *P. tabuliformis* [45] repress flowering in *A. thaliana*, suggesting their roles and potential as candidate genes to modulate life-cycle progression.

4. Conclusions

Taken together, our results show that *DAL1* can regulate other life-cycle events in addition to flowering, not only giving more functional information about *DAL1* with respect to the whole life cycle, but also providing potential targets for genetic modification to improve the reproductive traits of trees.

Author Contributions: Z.-L.Y. carried out the study, analyzed the data, and wrote the manuscript. D.-X.C. helped to carry out the study and analyze the data. Q.-L.Z. and X.-Y.L. helped to design and carry out the study. L.-W.Q. provided suggestions on the experimental design and analyses. W.-F.L. conceived and designed the study, helped to analyze the data, and revised the manuscript. All authors have read and agreed to the published version of the manuscript.

Institutional Review Board Statement: Not applicable.

Informed Consent Statement: Not applicable.

Data Availability Statement: All RNA-seq data in this study have been deposited in the NCBI SRA database with the accession number SAMN28416508.

Conflicts of Interest: The authors declare no conflict of interest.

References

1. Ma, J.J.; Chen, X.; Song, Y.T.; Zhang, G.F.; Zhou, X.Q.; Que, S.P.; Mao, F.; Pervaiz, T.; Lin, J.X.; Li, Y.; et al. MADS-box transcription factors MADS11 and DAL1 interact to mediate the vegetative-to-reproductive transition in pine. *Plant Physiol.* **2021**, *187*, 247–262. [CrossRef]
2. Shi, S.; Yan, S.; Zhao, C.; Zhang, P.; Yang, L.; Wang, C.; Shen, H. Deep sequencing and analysis of transcriptomes of *Pinus koraiensis* Sieb. & Zucc. *Forests* **2020**, *11*, 350.
3. Xiang, W.B.; Li, W.F.; Zhang, S.G.; Qi, L.W. Transcriptome-wide analysis to dissect the transcription factors orchestrating the phase change from vegetative to reproductive development in *Larix kaempferi*. *Tree Genet. Genomes* **2019**, *15*, 68. [CrossRef]
4. Zhang, Y.; Zang, Q.L.; Qi, L.W.; Han, S.Y.; Li, W.F. Effects of cutting, pruning, and grafting on the expression of age-related genes in *Larix kaempferi*. *Forests* **2020**, *11*, 218. [CrossRef]
5. Carlsbecker, A.; Tandre, K.; Johanson, U.; Englund, M.; Engström, P. The MADS-box gene *DAL1* is a potential mediator of the juvenile-to-adult transition in Norway spruce (*Picea abies*). *Plant J.* **2004**, *40*, 546–557. [CrossRef]
6. Katahata, S.I.; Futamura, N.; Igasaki, T.; Shinohara, K. Functional analysis of *SOC1*-like and *AGL6*-like MADS-box genes of the gymnosperm *Cryptomeria japonica*. *Tree Genet. Genomes* **2014**, *10*, 317–327. [CrossRef]
7. Bradley, D.; Ratcliffe, O.; Vincent, C.; Carpenter, R.; Coen, E. Inflorescence commitment and architecture in *Arabidopsis*. *Science* **1997**, *275*, 80–83. [CrossRef]

8.　Gatsuk, L.E.; Smirnova, O.V.; Vorontzova, L.I.; Zaugolnova, L.B.; Zhukova, L.A. Age states of plants of various growth forms: A review. *J. Ecol.* **1980**, *68*, 675–696. [CrossRef]

9.　Wang, B.; Smith, S.M.; Li, J. Genetic regulation of shoot architecture. *Annu. Rev. Plant Biol.* **2018**, *69*, 437–468. [CrossRef]

10.　Zhu, Y.; Wagner, D. Plant inflorescence architecture: The formation, activity, and fate of axillary meristems. *Cold Spring Harb. Perspect. Biol.* **2020**, *12*, a034652. [CrossRef]

11.　Merelo, P.; González-Cuadra, I.; Ferrándiz, C. A cellular analysis of meristem activity at the end of flowering points to cytokinin as a major regulator of proliferative arrest in *Arabidopsis*. *Curr. Biol.* **2022**, *32*, 749–762.e3. [CrossRef]

12.　Balanzà, V.; Martínez-Fernández, I.; Sato, S.; Yanofsky, M.F.; Ferrándiz, C. Inflorescence meristem fate is dependent on seed development and FRUITFULL in *Arabidopsis thaliana*. *Front. Plant Sci.* **2019**, *10*, 1622. [CrossRef]

13.　Balanzà, V.; Martinez-Fernández, I.; Sato, S.; Yanofsky, M.F.; Kaufmann, K.; Angenent, G.C.; Bemer, M.; Ferrándiz, C. Genetic control of meristem arrest and life span in *Arabidopsis* by a *FRUITFULL-APETALA2* pathway. *Nat. Commun.* **2018**, *9*, 565. [CrossRef]

14.　Hensel, L.L.; Nelson, M.A.; Richmond, T.A.; Bleecker, A.B. The fate of inflorescence meristems is controlled by developing fruits in *Arabidopsis*. *Plant Physiol.* **1994**, *106*, 863–876. [CrossRef]

15.　Martínez-Fernández, I.; Menezes de Moura, S.; Alves-Ferreira, M.; Ferrándiz, C.; Balanzà, V. Identification of players controlling meristem arrest downstream of the FRUITFULL-APETALA2 pathway. *Plant Physiol.* **2020**, *184*, 945–959. [CrossRef]

16.　Cao, S.; Luo, X.; Xu, D.; Tian, X.; Song, J.; Xia, X.; Chu, C.; He, Z. Genetic architecture underlying light and temperature mediated flowering in Arabidopsis, rice, and temperate cereals. *New Phytol.* **2021**, *230*, 1731–1745. [CrossRef]

17.　Ye, L.X.; Zhang, J.X.; Hou, X.J.; Qiu, M.Q.; Wang, W.F.; Zhang, J.X.; Hu, C.G.; Zhang, J.Z. A MADS-Box gene *CiMADS43* is involved in citrus flowering and leaf development through interaction with CiAGL9. *Int. J. Mol. Sci.* **2021**, *22*, 5205. [CrossRef]

18.　Zhao, H.; Lin, K.; Ma, L.; Chen, Q.; Gan, S.; Li, G. Arabidopsis NUCLEAR FACTOR Y A8 inhibits the juvenile-to-adult transition by activating transcription of MIR156s. *J. Exp. Bot.* **2020**, *71*, 4890–4902. [CrossRef]

19.　Bolger, A.M.; Lohse, M.; Usadel, B. Trimmomatic: A flexible trimmer for Illumina sequence data. *Bioinformatics* **2014**, *30*, 2114–2120. [CrossRef]

20.　Trapnell, C.; Williams, B.A.; Pertea, G.; Mortazavi, A.; Kwan, G.; van Baren, M.J.; Salzberg, S.; Wold, B.J.; Pachter, L. Transcript assembly and quantification by RNA-seq reveals unannotated transcripts and isoform switching during cell differentiation. *Nat. Biotechnol.* **2010**, *28*, 511–515. [CrossRef]

21.　Love, M.I.; Huber, W.; Anders, S. Moderated estimation of fold change and dispersion for RNA-seq data with DESeq2. *Genome Biol.* **2014**, *15*, 550. [CrossRef] [PubMed]

22.　Benjamini, Y.; Hochberg, Y. Controlling the false discovery rate: A practical and powerful approach to multiple testing. *J. R. Stat. Soc. Ser. B* **1995**, *57*, 289–300. [CrossRef]

23.　Chen, C.; Chen, H.; Zhang, Y.; Thomas, H.R.; Frank, M.H.; He, Y.; Xia, R. TBtools: An integrative toolkit developed for interactive analyses of big biological data. *Mol. Plant* **2020**, *13*, 1194–1202. [CrossRef] [PubMed]

24.　Bergonzi, S.; Albani, M.C. Reproductive competence from an annual and a perennial perspective. *J. Exp. Bot.* **2011**, *62*, 4415–4422. [CrossRef]

25.　Ware, A.; Walker, C.H.; Šimura, J.; González-Suárez, P.; Ljung, K.; Bishopp, A.; Wilson, Z.A.; Bennett, T. Auxin export from proximal fruits drives arrest in temporally competent inflorescences. *Nat. Plants* **2020**, *6*, 699–707. [CrossRef]

26.　Freytes, S.N.; Canelo, M.; Cerdán, P.D. Regulation of flowering time: When and where? *Curr. Opin. Plant Biol.* **2021**, *63*, 102049. [CrossRef]

27.　Randoux, M.; Davière, J.M.; Jeauffre, J.; Thouroude, T.; Pierre, S.; Toualbia, Y.; Perrotte, J.; Reynoird, J.P.; Jammes, M.J.; Hibrand-Saint Oyant, L.; et al. RoKSN, a floral repressor, forms protein complexes with RoFD and RoFT to regulate vegetative and reproductive development in rose. *New Phytol.* **2014**, *202*, 161–173. [CrossRef]

28.　Yu, H.; Ito, T.; Wellmer, F.; Meyerowitz, E.M. Repression of AGAMOUS-LIKE 24 is a crucial step in promoting flower development. *Nat. Genet.* **2004**, *36*, 157–161. [CrossRef]

29.　Dorca-Fornell, C.; Gregis, V.; Grandi, V.; Coupland, G.; Colombo, L.; Kater, M.M. The Arabidopsis *SOC1*-like genes *AGL42*, *AGL71* and *AGL72* promote flowering in the shoot apical and axillary meristems. *Plant J.* **2011**, *67*, 1006–1017. [CrossRef]

30.　Kirik, V.; Kölle, K.; Wohlfarth, T.; Miséra, S.; Bäumlein, H. Ectopic expression of a novel *MYB* gene modifies the architecture of the *Arabidopsis* inflorescence. *Plant J.* **1998**, *13*, 729–742. [CrossRef]

31.　Chen, W.H.; Li, P.F.; Chen, M.K.; Lee, Y.I.; Yang, C.H. Forever Young Flower negatively regulates ethylene response DNA-binding factors by activating an ethylene-responsive factor to control Arabidopsis floral organ senescence and abscission. *Plant Physiol.* **2015**, *168*, 1666–1683. [CrossRef] [PubMed]

32.　Oh, S.A.; Lee, S.Y.; Chung, I.K.; Lee, C.H.; Nam, H.G. A senescence-associated gene of *Arabidopsis thaliana* is distinctively regulated during natural and artificially induced leaf senescence. *Plant Mol. Biol.* **1996**, *30*, 739–754. [CrossRef] [PubMed]

33.　Woo, H.R.; Kim, J.H.; Nam, H.G.; Lim, P.O. The delayed leaf senescence mutants of *Arabidopsis*, *ore1*, *ore3*, and *ore9* are tolerant to oxidative stress. *Plant Cell Physiol.* **2004**, *45*, 923–932. [CrossRef] [PubMed]

34.　Zhang, Z.; Li, W.; Gao, X.; Xu, M.; Guo, Y. DEAR4, a member of DREB/CBF family, positively regulates leaf senescence and response to multiple stressors in *Arabidopsis thaliana*. *Front. Plant Sci.* **2020**, *11*, 367. [CrossRef]

35.　Brunner, A.M.; Varkonyi-Gasic, E.; Jones, R.C. Phase change and phenology in trees. In *Comparative and Evolutionary Genomics of Angiosperm Trees*; Springer: Berlin/Heidelberg, Germany, 2017; pp. 227–274.

36. Flachowsky, H.; Szankowski, I.; Waidmann, S.; Peil, A.; Tränkner, C.; Hanke, M.V. The *MdTFL1* gene of apple (*Malus* × *domestica* Borkh.) reduces vegetative growth and generation time. *Tree Physiol.* **2012**, *32*, 1288–1301. [CrossRef]

37. Haberman, A.; Ackerman, M.; Crane, O.; Kelner, J.J.; Costes, E.; Samach, A. Different flowering response to various fruit loads in apple cultivars correlates with degree of transcript reaccumulation of a TFL1-encoding gene. *Plant J.* **2016**, *87*, 161–173. [CrossRef]

38. Yamagishi, N.; Kishigami, R.; Yoshikawa, N. Reduced generation time of apple seedlings to within a year by means of a plant virus vector: A new plant-breeding technique with no transmission of genetic modification to the next generation. *Plant Biotechnol. J.* **2014**, *12*, 60–68. [CrossRef]

39. Zuo, X.; Xiang, W.; Zhang, L.; Gao, C.; An, N.; Xing, L.; Ma, J.; Zhao, C.; Zhang, D. Identification of apple TFL1-interacting proteins uncovers an expanded flowering network. *Plant Cell Rep.* **2021**, *40*, 2325–2340. [CrossRef]

40. Freiman, A.; Shlizerman, L.; Golobovitch, S.; Yablovitz, Z.; Korchinsky, R.; Cohen, Y.; Samach, A.; Chevreau, E.; Le Roux, P.M.; Patocchi, A.; et al. Development of a transgenic early flowering pear (*Pyrus communis* L.) genotype by RNAi silencing of *PcTFL1-1* and *PcTFL1-2*. *Planta* **2012**, *235*, 1239–1251. [CrossRef]

41. Yamagishi, N.; Li, C.; Yoshikawa, N. Promotion of flowering by *Apple Latent Spherical Virus* vector and virus elimination at high temperature allow accelerated breeding of apple and pear. *Front. Plant Sci.* **2016**, *7*, 171. [CrossRef]

42. Mohamed, R.; Wang, C.T.; Ma, C.; Shevchenko, O.; Dye, S.J.; Puzey, J.R.; Etherington, E.; Sheng, X.; Meilan, R.; Strauss, S.H.; et al. *Populus CEN/TFL1* regulates first onset of flowering, axillary meristem identity and dormancy release in *Populus*. *Plant J.* **2010**, *62*, 674–688. [CrossRef] [PubMed]

43. Karlgren, A.; Gyllenstrand, N.; Kälman, T.; Sundström, J.F.; Moore, D.; Lascoux, M.; Lagercrantz, U. Evolution of the PEBP gene family in plants: Functional diversification in seed plant evolution. *Plant Physiol.* **2011**, *156*, 1967–1977. [CrossRef] [PubMed]

44. Liu, Y.Y.; Yang, K.Z.; Wei, X.X.; Wang, X.Q. Revisiting the phosphatidylethanolamine-binding protein (PEBP) gene family reveals cryptic *FLOWERING LOCUS T* gene homologs in gymnosperms and sheds new light on functional evolution. *New Phytol.* **2016**, *212*, 730–744. [CrossRef] [PubMed]

45. Niu, S.H.; Li, J.; Bo, W.H.; Yang, W.F.; Zuccolo, A.; Giacomello, S.; Chen, X.; Han, F.X.; Yang, J.H.; Song, Y.T.; et al. The Chinese pine genome and methylome unveil key features of conifer evolution. *Cell* **2022**, *185*, 204–217.e214. [CrossRef]